

Supporting Information

Ionic Liquid-based Low-dimensional Fluorosensor for Ultrasensitive Detection of Perchlorate ions in Aqueous Media

Subekchha Pradhan, and Sudhir Kumar Das*

Department of Chemistry, University of North Bengal, Raja Rammohunpur, Darjeeling, West Bengal-734013, India

Corresponding author: (Dr. S. K. Das; E-mail: sudhirkumardas@nbu.ac.in)

Table of contents

Sl. No.	Descriptions	Page No.
Figure. S1	¹ H NMR spectrum (CDCl ₃ , 400 MHz) of parent moiety, C.	2
Figure. S2	High-resolution mass spectra of the parent moiety, C.	3
Figure S3	¹ H NMR spectrum (CDCl ₃ , 400 MHz) of sodium salt, D.	3
Figure. S4	High-resolution mass spectra of the sodium salt of the parent moiety, D.	4
Figure. S5	¹ H NMR spectrum (CDCl ₃ , 400 MHz) of APIL .	5
Figure. S6	¹³ C NMR spectrum (CDCl ₃ , 100 MHz) of APIL .	5
Figure. S7	³¹ P NMR spectrum (CDCl ₃ , 400 MHz) of APIL .	6
Figure S8	LCMS spectra of APIL ; (A) positive ion mode and (B) negative ion mode.	6-7
Figure S9	(a) Differential scanning calorimetry (DSC) thermogram of APIL . (b) Thermogravimetric analysis (TGA) thermogram of APIL	8
Figure S10	Zeta potential of the nano-GUMBOS, APIL	8
Figure S11	UV-visible absorption spectra of optode APIL in different percentages of water. (b) Fluorescence spectra of APIL in water-DMSO-D6 mixed solvents demonstrating ACQ.	9
Figure S12	(a) UV vis spectroscopy comparison of parent moiety and parent moiety on addition of ClO ₄ ⁻ (b) Photoluminescence comparison of parent moiety and parent moiety upon addition of ClO ₄ ⁻	9
Figure S13	(a) UV-visible absorption spectral comparison of sodium salt and sodium salt on addition of ClO ₄ ⁻ (b) Photoluminescence comparison of sodium salt and sodium salt upon addition of ClO ₄ ⁻	10
Figure S14	Histogram displaying the selectivity of mAPIL (43 μM) with ClO ₄ ⁻ over other metals (45 μM).	10
Figure S15	(a) Fluorometric stability of mAPIL suspension. (b) Fluorometric response time of water-suspended mAPIL for the detection of ClO ₄ ⁻ .	11
Table S1	Solvatochromism comparison of the parent moiety, its sodium	11-12

	salt, and ionic liquid	
Table S2	Calculated ΔG values at various temperatures	12
Table S3	Determination of ClO_4^- ions in various water samples.	12
Figure S16	Influence of pH on the photoluminescence behavior of mAPIL in the absence and presence of ClO_4^- ions.	13
Table S4	Comparison table of different chemosensors that have been introduced for detecting ClO_4^- ions in the last few decades, with our prepared mAPIL .	13-14

S1 Experimental section

S1.1. Synthetic procedures and characterizations.

Compound C: Imidazole derivative compound **c** was synthesized via a multistep procedure. 9, 10-Phenanthrenequinone (**a**) (150 mg) was dissolved in glacial acetic acid (AcOH) and reacted with ammonium acetate at 90 °C for 30 min, followed by the addition of anthracene-9-carbaldehyde (**b**) (200 mg, 1 equiv). The mixture was refluxed at 110 °C for 90 min, yielding yellow powder imidazole derivative (**c**) upon precipitation in ice water (78% yield after medium-pressure liquid chromatography (MPLC) purification, 15% EtOAc/petroleum ether). **¹H NMR** (400 MHz, CDCl_3) δ 8.957- 8.94 (m, 3H), 8.601 (d, 1H), 8.392 (d, 1H). 8.257 (d, 2H), 7.815 (d, 2H), 7.722 (m, 4H), 7.616 (t, 2H), 7.546 (t, 2H), 13.9 (s, 1H, NH). HRMS calculated for $\text{C}_{29}\text{H}_{18}\text{N}_2$: 394.47, found: 395.15 (m/z).

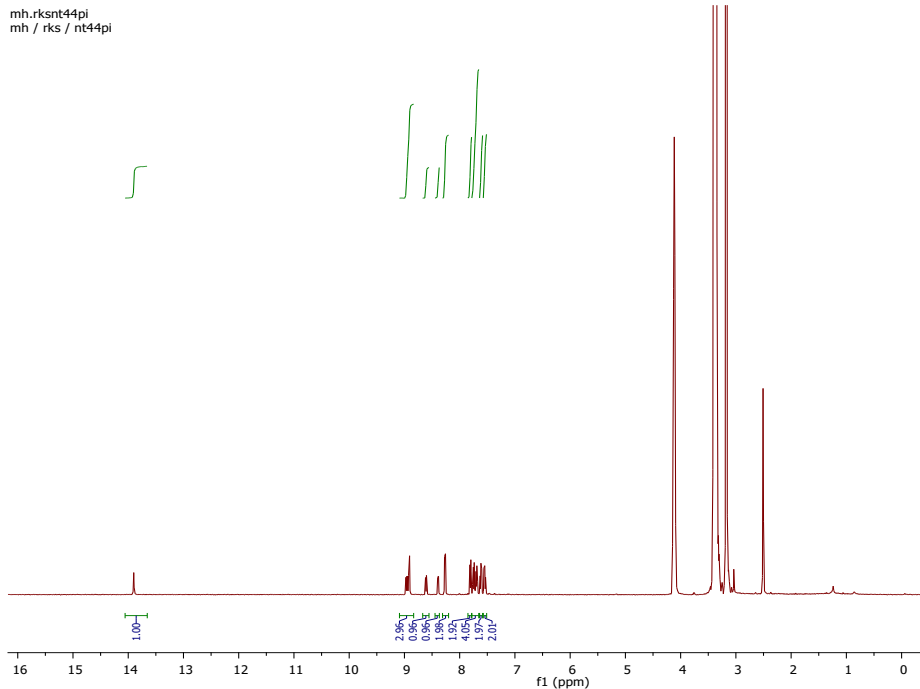


Figure S1: ^1H NMR spectrum (CDCl_3 , 400 MHz) of parent moiety, C.

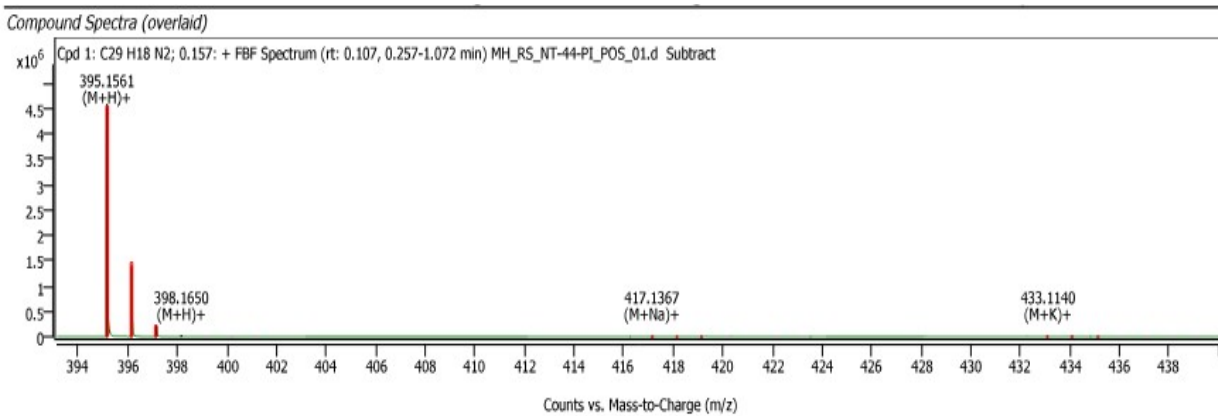


Figure S2: High-resolution mass spectra of parent moiety, C.

Compound D: Compound c was treated with NaOH in methanol, stirred for 6 h, and evaporated to afford Sodium salt intermediate D. ^1H NMR (400 MHz, CDCl_3) δ 7.707-7.671 (m, 5H), 7.375-7.346 (m, 4H), 6.286 (d, 2H), 6.185 (s, 2H), 6.082 (s, 4H). HRMS calculated for $\text{C}_{29}\text{H}_{17}\text{N}_2\text{Na}$: 416.47, found: 417.13 (m/z).

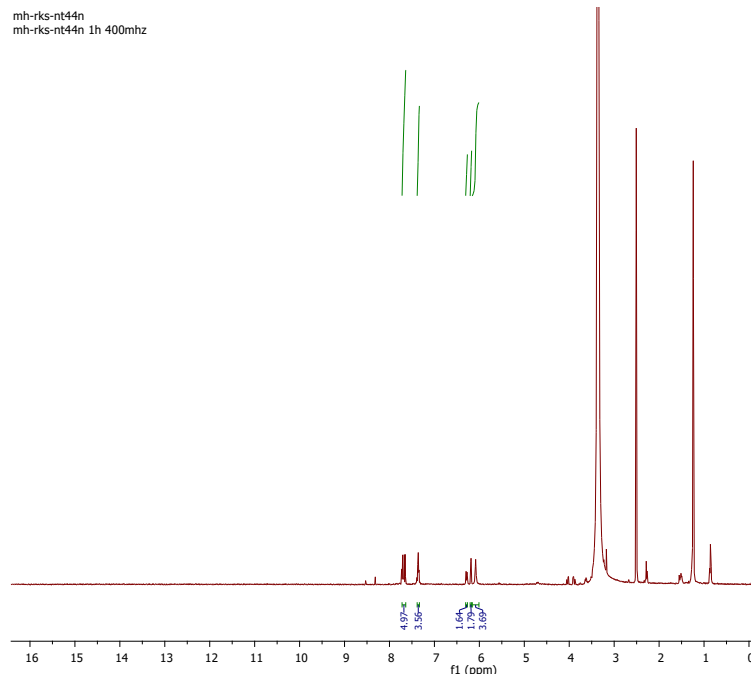


Figure S3: ^1H NMR spectrum (CDCl_3 , 400 MHz) of sodium salt, D.

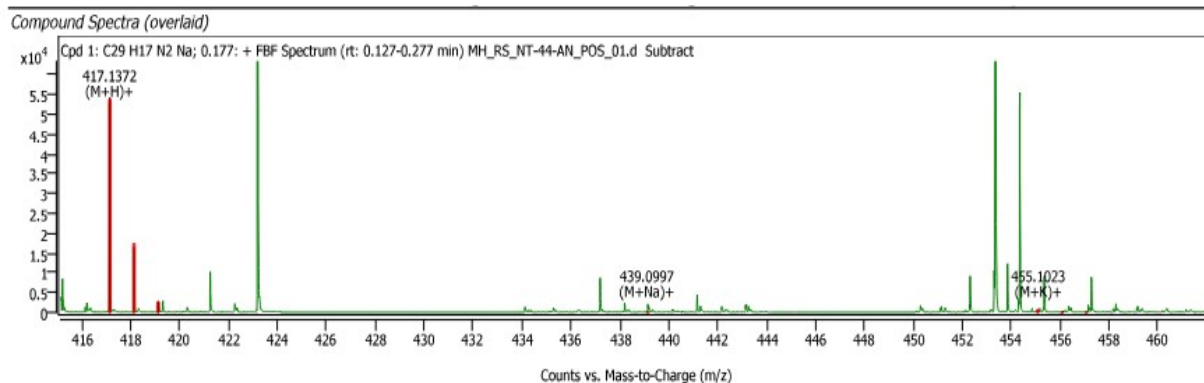


Figure S4: High-resolution mass spectra of the sodium salt of the parent moiety, D.

Ionic Liquid (APIL): APIL was synthesized following a literature method with slight modifications¹. Succinctly, in a dichloromethane (DCM)-water mixture of 2:1(v/v), the sodium salt D and the ionic liquid $\text{P}_{66614}\text{Cl}$ in a 1:1 molar ratio were stirred overnight, resulting in an ion exchange process. The solvent phase was purged, and repeated washing of the DCM layer with water was performed to remove the NaCl byproduct, which was confirmed by adding AgNO_3

solution and washing the reaction mixture multiple times until no white precipitate of AgCl formed. To eliminate the trace water in the DCM layer containing APIL, it was passed through anhydrous Na₂SO₄. **APIL** was obtained (SCHEME 1) by evaporating the DCM and residual water under vacuum at 60°C for 2 hours ¹H NMR (400 MHz, DMSO, δ(ppm)):7.684(s,1H), 7.564-7.479 (m,3H), 7.708 (m,4H), 7.892-7.777 (q,2H), 8.062-7.892 (m,2H), 8.294-8.136 (m,2H), 8.501-5.324 (d,1H), 8.880-8.693 (m,1H), 8.991-8.896 (m,1H), 2.183-2.178 (m,19H), 1.387-1.381 (m,20H), 0.866-0.8605 (m,21H) ¹³C NMR (100 MHz, CDCl₃, δ (ppm)): 199.11, 198.42, 196.33 ,196.02, 194.98, 193.76,192.78, 191.95, 191.16, 173.46, 162.22 ,160.90, 159.54, 148.72, 140.37, 140.09, 139.19, 137.84, 128.84, 122.35, 121.51, 118.39, 111.86, 110.86, 106.39, 102.78, 101.88 ,99.78, 93.55 71.62, 69.76, 67.68, 67.41, 66.68, 66.07, 65.95, 65.4, 63.10, 57.45, 57.40, 56.61, 55.81, 54.96, 53.34, 32.84, 31.75, 31.47, 31.33, 29.15, 23.13, 22.55, 21.44, 14.42, 8.25, 4.53, 4.06, 2.47, 1.58, 0.18, 0.93. ³¹P NMR (400 MHz, CDCl₃, δ (ppm): 34.9

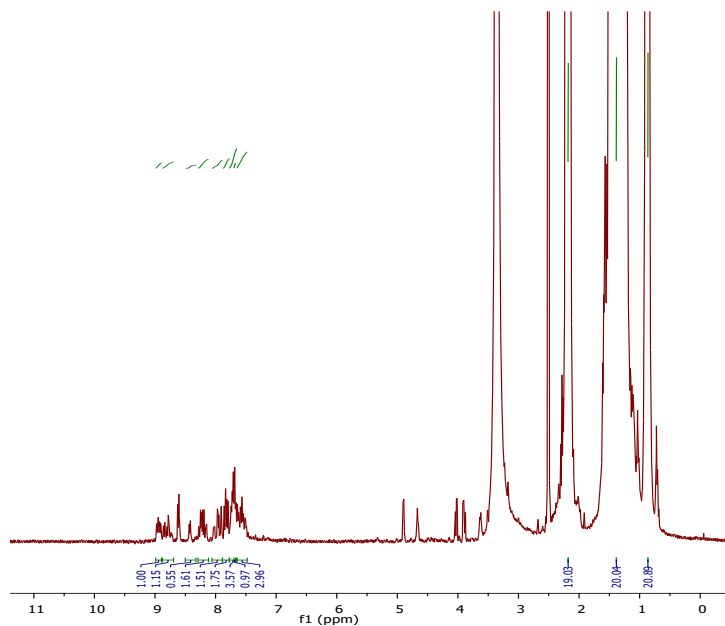


Figure. S5: ¹H NMR spectrum (CDCl₃, 400 MHz) of **APIL**.

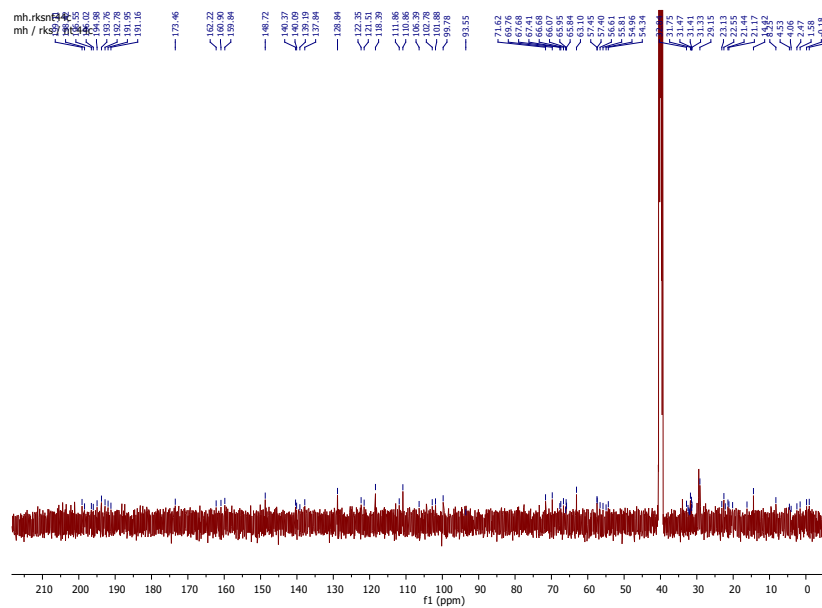


Figure. S6: ^{13}C NMR spectrum (CDCl_3 , 100 MHz) of APIL.

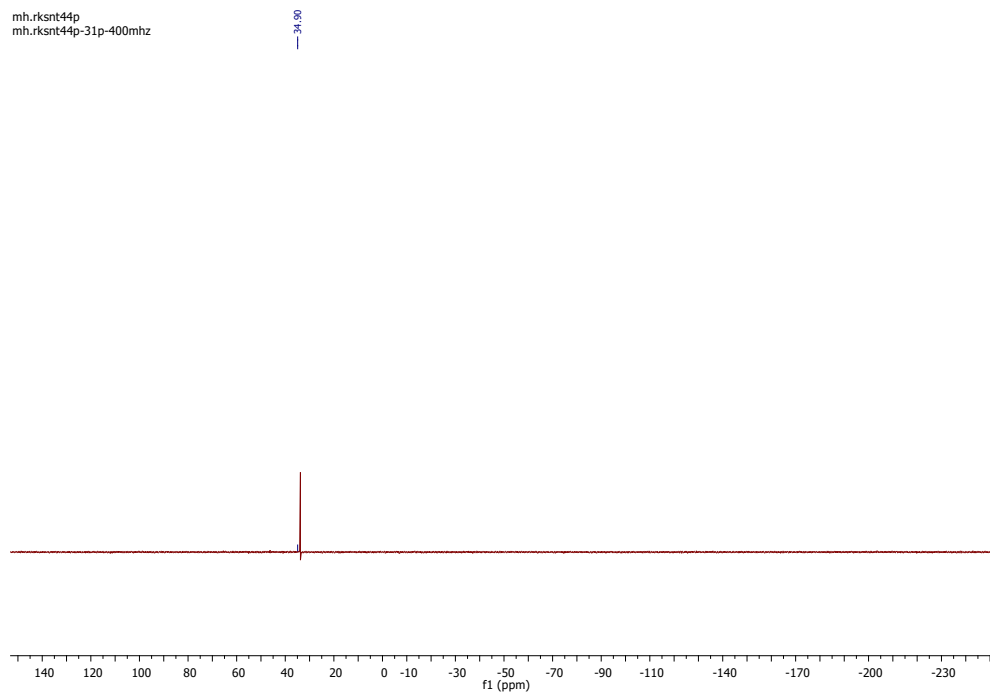


Figure. S7: ^{31}P NMR spectrum (CDCl_3 , 400 MHz) of APIL.

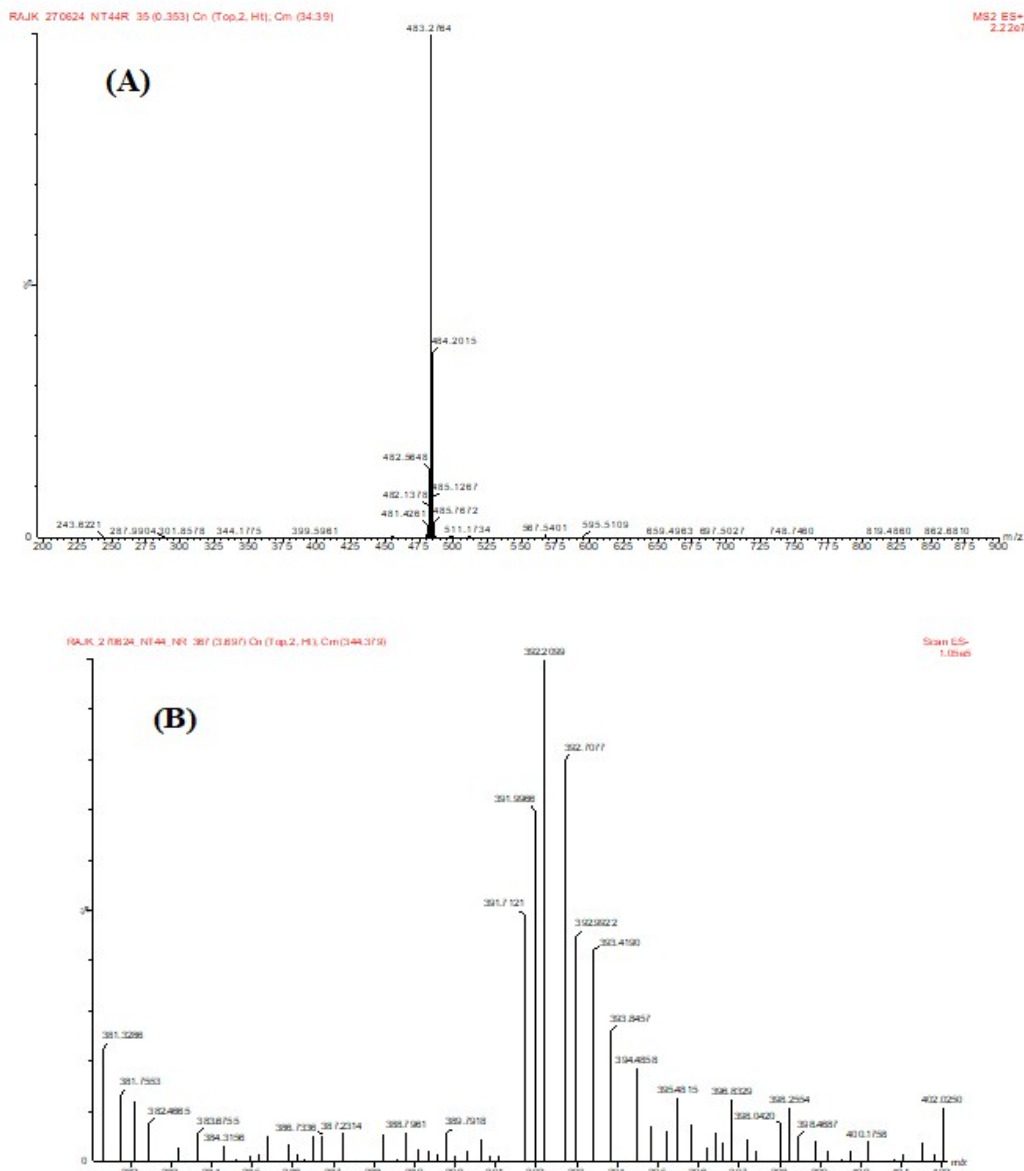


Figure. S8: LCMS spectra of APIL; (A) positive ion mode and (B) negative ion mode.

S1.2. Estimation of Quantum Yield

For the determination of the fluorescence quantum yield (Φ_x) of **mAPIL** in DMSO, and to investigate the aggregation-caused quenching (ACQ) mechanism by increasing the water fraction, quinine sulfate in 0.1 N H_2SO_4 ($\Phi = 0.55$)² was used as the standard.

$$\Phi = \Phi_c \left(\frac{F_s}{F_c} \right) \left(\frac{A_c}{A_s} \right) \left(\frac{\eta_s^2}{\eta_c^2} \right)$$

In the applied formula, Φ indicates quantum yield, F is the integrated fluorescence emission, A is absorbance, and η is the refractive index of the solvent. The subscripts "c" and "s" denote the standard and the sample (APIL in DMSO / mAPIL / mAPIL - ClO₄⁻), respectively. Based on this analysis, the quantum yields of APIL in DMSO, mAPIL, and its ClO₄⁻ complex were found.

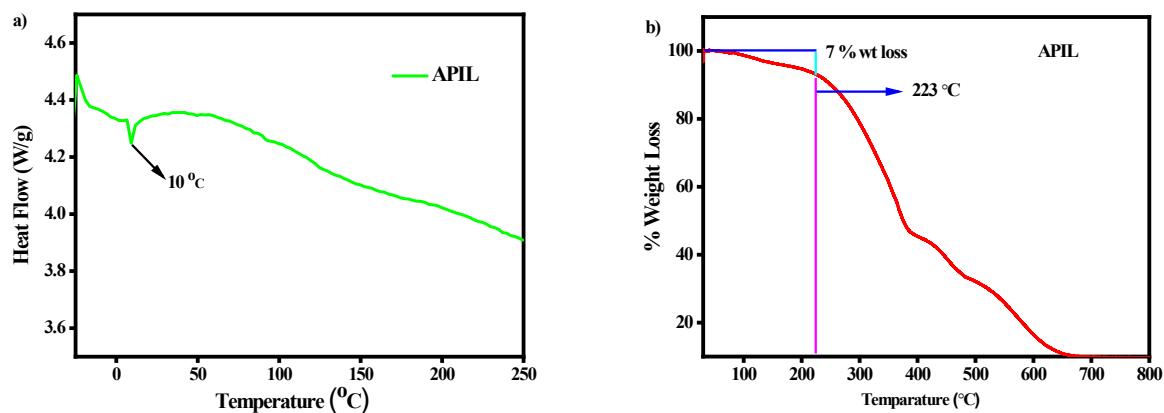


Figure S9: (a) Differential scanning calorimetry (DSC) thermogram of APIL. (b) Thermogravimetric analysis (TGA) thermogram of APIL

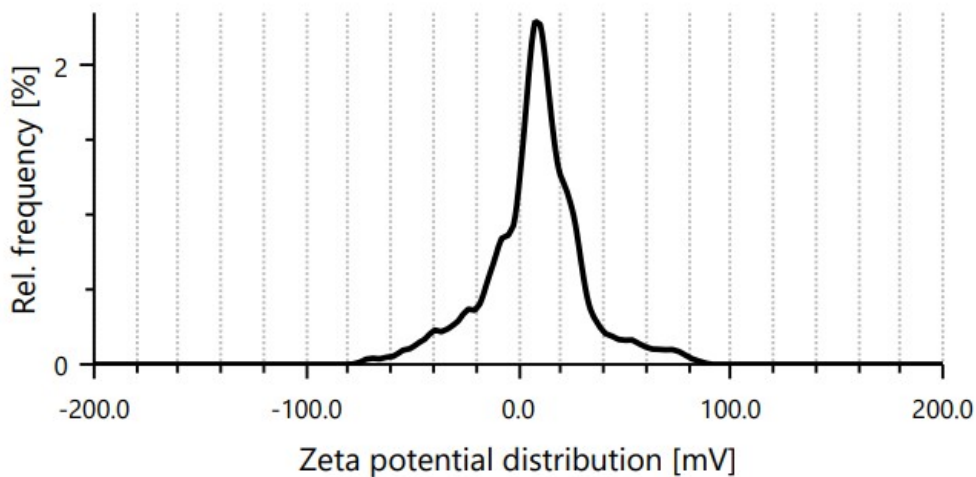


Figure S10: Zeta potential of the mAPIL solution.

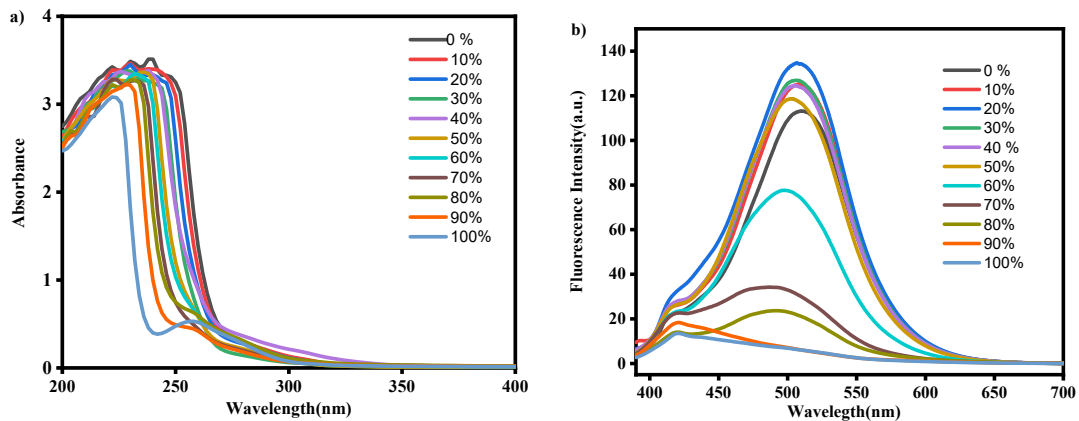


Figure. S11 (a)UV-visible absorption spectra of optode **APIL** in different percentages of water. (b) Fluorescence spectra of **APIL** in water-DMSO mixed solvents demonstrating ACQ.

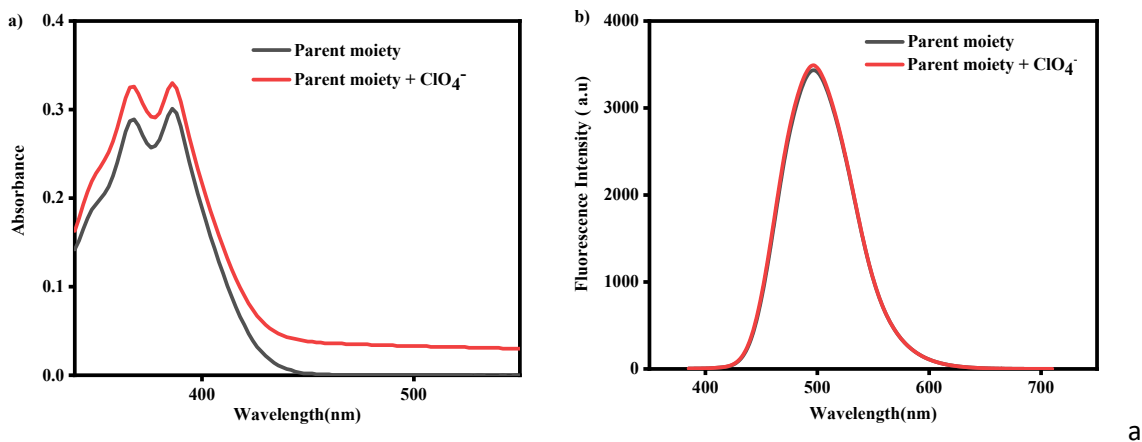


Figure S12: (a)UV vis spectroscopy comparison of parent moiety and parent moiety on addition of ClO_4^- (b) Photoluminescence comparison of parent moiety and parent moiety upon addition of ClO_4^-

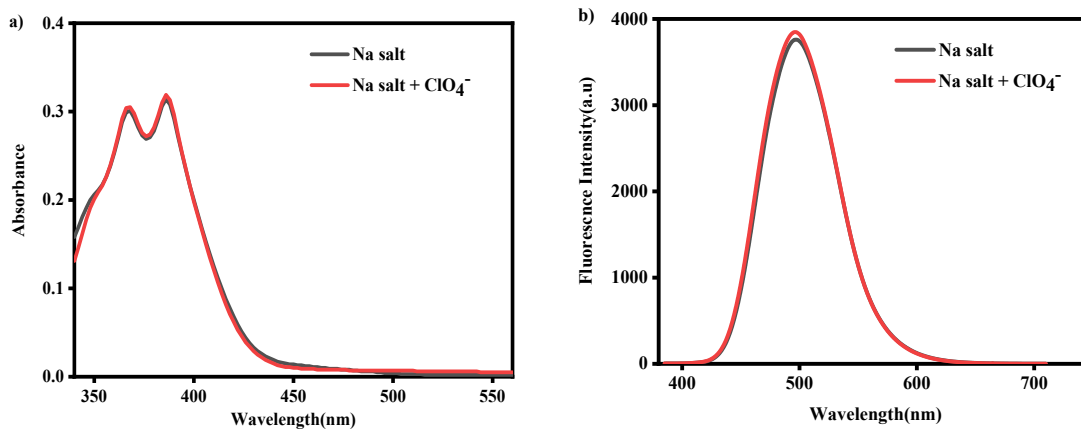


Figure S13: (a) UV-visible spectral comparison of sodium salt and sodium salt on the addition of ClO₄⁻ ions. (b) Photoluminescence comparison of sodium salt and sodium salt upon addition of ClO₄⁻

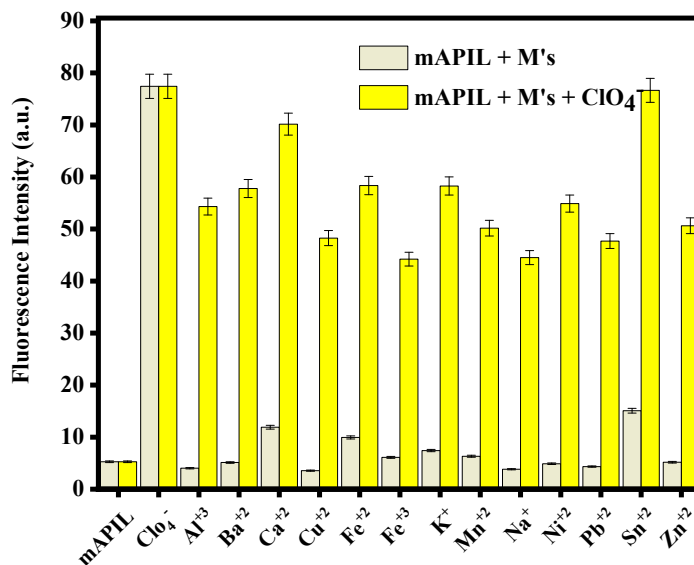


Figure S14: Histogram displaying the selectivity of mAPIL (43 μM) with ClO₄⁻ ions over other metals (45 μM).

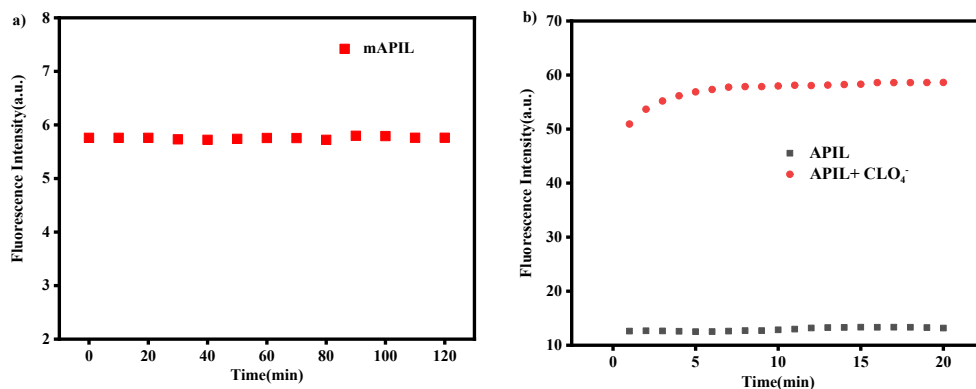


Figure S15: (a) Fluorometric stability of **mAPIL** suspension. (b) Fluorometric response time of water-suspended **mAPIL** for the detection of ClO_4^- ions.

Table S1: Solvatochromism comparison of the parent moiety, its sodium salt, and ionic liquid

Parent Moiety	Solvent	UV(nm)	FL(nm)
	THF	384	487.8
	DCM	386	492.4
	DMF	387	494.6
	DMSO	388	496.2
	WATER	390	490.4
Sodium Salt	Solvent	UV	FL
	THF	306	487.6
	DCM	366	493.4
	DMF	386	495.6
	DMSO	388	496.4
	WATER	392	491
APIL	Solvent	UV	FL
	THF	264.43	498.6

APIL	DCM	276	500
	DMF	280	502
	DMSO	284	508.61
	WATER	294.5	421.6

Table S2: Calculated ΔG values at various temperatures.

Temperature(°C)	ΔG (Jmol⁻¹)	ΔH (Jmol⁻¹)	ΔS (Jmol⁻¹ K⁻¹)
15	-22926.64	-21732.54	79.61
25	-23722.71		
35	-24518.77		
45	-25314.83		
55	-26110.9		
65	-26906.96		

Table S3: Determination of ClO₄⁻ ions in various water samples.

Sample	Added (μM)	Found (μM)	Recovery (%)
River water	7.29	7.23	99.09
	9.7	9.5	97.85
	12.1	11.94	98.68
	14.49	14.45	99.70
	16.86	16.56	98.19
	19.23	18.9	98.50
	21.5	21.40	99.17
Municipalitywater	12.1	11.8	98.12
	14.49	14.28	98.55
	19.23	18.9	98.3
	21.58	21.54	99.83
	23.92	23.72	99.18
	26.25	26.17	99.69
	28.57	28.40	99.42

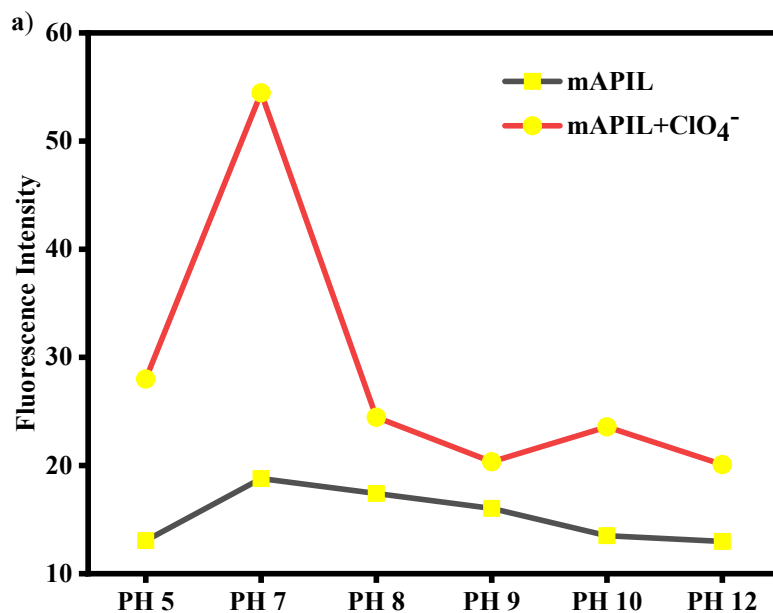


Figure S16: Influence of pH on the photoluminescence behavior of **mAPIL** in the absence and presence of ClO_4^- ions.

Table S4: Comparison table of different chemosensors that have been introduced for detecting ClO_4^- ion in the last few decades, with our prepared **mAPIL**

Structure	Medium	Optical signaling	LOD	Ref. No.
Methylene Blue–Modified gold nanoparticles	Ultrapure water	Colorimetric	24 μM	3
[Pt(terpy)Br]-PVA hydrogel sensor	acetic acid/water/ethanol (0.5:1:1, v/v) mixed solution	turn-on luminescence	25 nM	4
1-(4-Biphenyl)benzimidazolium based dipodal system	HEPES buffer (0.01 M)	quenching of fluorescence intensity	100 nM	5
Ion-selective electrodes	water	-	10 ^{-7.4} M	6

using multi-walled carbon nanotubes as ion-to-electron transducers					
1-(2-(3', 6'-bis(diethylamino)-3-oxospiro[isoinoline-1,9'-xanthene]-2-yl)ethyl)thiourea	HEPES buffer (0.1 M in CH ₃ CN/water, 4/1, v/v, pH 7.4)	colorimetric and fluorimetric	1×10^{-7} M.	7	
perylene diimide based chemosensor	HEPES buffer (10% DMSO) (v/v) (pH 7.4)	fluorescence quenching	60 nM	8	
Benzoimidazole-based	HEPES buffer – 2% DMSO, pH 7.4	fluorescence based	1.6 μ M	9	
CHEMFET devices based on plasticized PVC membranes containing the phosphadithiamacrocycle.	-	Potentiometrically	3×10^{-7} M	10	
ISE devices based on plasticized PVC membranes containing the phosphadithiamacrocycle.	-	Potentiometrically	8×10^{-7} M	10	
gold–silica composite nanoparticle substrates for perchlorate	-	surface-enhanced Raman spectroscopy	10^{-6} M	11	
Novel polymeric membrane (PME) electrodes based on a phosphorous(V)-tetraphenylporphyrin complex.	Acetonitrile	UV-Vis, Fluorescence, and Potentiometrically	5 μ M	12	

Coated glassy carbon (CGCE) electrodes based on a phosphorous(V)-tetraphenylporphyrin complex.	Acetonitrile	UV-Vis, Fluorescence, and Potentiometrically.	0.7 μ M	12
Anthracene phenantroimidazolate-based ionic liquid	Water	fluorometric	12.7 nM	This work

- 1 W. I. S. Galpothdeniya, K. S. McCarter, S. L. De Rooy, B. P. Regmi, S. Das, F. Hasan, A. Tagge en I. M. Warner, *RSC Adv.*, 2014, **4**, 7225–7234.
- 2 J. Drobnik en E. Yeagers, *J. Mol. Spectrosc.*, 1966, **19**, 454–455.
- 3 B. Keskin, A. Üzer en R. Apak, *Talanta*, 2020, **206**, 120240.
- 4 Z. Su, Y. Li, J. Li en X. Dou, *Sensors Actuators B Chem.*, 2021, **336**, 129728.
- 5 R. Kumar, S. Kumar, P. Singh, G. Hundal, M. S. Hundal en S. Kumar, *Analyst*, 2012, **137**, 4913–4916.
- 6 E. J. Parra, G. A. Crespo, J. Riu, A. Ruiz en F. X. Rius, *Analyst*, 2009, **134**, 1905–1910.
- 7 A. Sahana, A. Banerjee, S. Lohar, A. Chottapadhyay, S. K. Mukhopadhyay en D. Das, *RSC Adv.*, 2013, **3**, 14044–14047.
- 8 P. Singh, L. S. Mittal, V. Vanita, R. Kumar, G. Bhargava, A. Walia en S. Kumar, *Chem. Commun.*, 2014, **50**, 13994–13997.
- 9 R. Kumar, S. Sandhu, P. Singh en S. Kumar, *J. Mater. Chem. C*, 2016, **4**, 7420–7429.
- 10 J. Casabó, L. Escriche, C. Pérez-Jiménez, J. A. Muñoz, F. Teixidor, J. Bausells en A.

- Errachid, *Anal. Chim. Acta*, 1996, **320**, 63–68.
- 11 W. Wang, C. Ruan en B. Gu, *Anal. Chim. Acta*, 2006, **567**, 121–126.
- 12 M. Shamsipur, A. Soleymanpour, M. Akhond, H. Sharghi en A. R. Hasaninejad, *Sensors Actuators B: Chem.*, 2003, **89**, 9–14.